p-ISSN 2089 – 0133 e-ISSN 2477-6416
URL: https://jurnal.uns.ac.id/ijap/article/view/61501

Indonesian Journal of Applied Physics (IJAP) Vol. 15 No. 1 page 1
DOI: https://doi.org/10.13057/ijap.v15i1.61501

INTERPRETATION OF 3-D MAGNETIC INVERSION RESULTS IN THE MAJENANG AREA, INDONESIA

Accep Handyarso*[1,2]

[1] Research Center for Geological Resources (RCGR), National Research and Innovation Agency (NRIA) of the Republic of Indonesia. Samaun Samadikun Science and Technology CenterBandung, Indonesia.

[2] Ex-Center for Geological Survey, Geological Agency, Ministry of Energy and Mineral Resources (MEMR) of the Republic of Indonesia, Bandung, Indonesia.

*accep.handyarso@brin.go.id

Received 27-05-2022, Revised 20-10-2023, Accepted 02-04-2023,
Available Online 01-04-2025, Published Regularly April 2025

ABSTRACT

The Total Magnetic Intensity (TMI) data requires conversion using Reduction to Pole (RTP) or Reduction to Equator (RTE) filters prior to the interpretation process. However, the low latitude location causes stability issue in the RTP and is replaced by the RTE computing processes. Noteworthy, the RTE results have inverted polarity. An inverse modeling scheme based on direct use of TMI data using equivalent-source provides an alternative solution to address this issue. In this research, synthetic modeling of a strike-slip fault geometry is conducted to assist the interpretation process in order to guide during recognizing similar anomaly contour patterns in field datasets. TMI data interpretation was conducted in a volcanic area located in Majenang, Central Java. According to the research findings, a dextral strike-slip fault with a northwest-southeast lineament is delineated. This fault is interpreted as part of the Pamanukan-Cilacap Fault Zone (PCFZ). Additionally, a circular anomaly is exposed and inferred to be the edge of ancient-volcanic-caldera (ring-fault or caldera-rims) in the study area. Both results were confirmed through a comparison of geomagnetic and gravity data. The high-susceptibility zone correlates well with the high-density zone and the outcrop of the Sangkur Volcano's intrusion body, which is inferred precedes the intrusion body of the Kumbang Volcano. The intrusive bodies located around the PCFZ manifest the presence of a weak zone that has been intruded by magmatism, contributing to the formation of volcanoes along the fault as a volcano-tectonic setting in the area.

Keywords: Geomagnetic; gravity; strike-slip fault; volcano-tectonic; Central Java

Cite this as: Handyarso, A. 2025. Interpretation of 3-D Magnetic Inversion Results in The Majenang Area, Indonesia. *IJAP: Indonesian Journal of Applied Physics, 15*(1), 1-16. doi: https://doi.org/10.13057/ijap.v15i1.61501

INTRODUCTION

Geomagnetic surveying is frequently utilized as an initial geophysical study in the preliminary stages of geological-geophysical research. Magnetic methods facilitate the rapid mapping of magnetic susceptibility distribution beneath the surface, allowing for the mapping of large areas in relatively short time periods. The geomagnetic method is capable of delineating geological structures caused by the lateral lithological changes of magnetized rocks beneath the Earth's surface [1]. However, a stability issue is faced during the conversion of the Total Magnetic Intensity (TMI) datasets into Reduction to Pole (RTP) due to low latitude survey location. Thus, Reduction to Equator (RTE) emerged as a solution in such location even though the RTE calculation result provides an inverted polarity. Equivalent sources provide another alternative solution to address stability issue in the 3-D magnetic data inversion as demonstrated in this study.

Integrating magnetic and gravity methods can mitigate ambiguity problems during the data interpretation process. Geological modeling of strike-slip faults is conducted based on these two methods. Modeling effort is designed to guide in recognizing anomaly contour patterns of the field datasets. The magnetic method is also effective for delineating igneous or intrusive rocks as well as identification of the fault discontinuity in the sedimentary rock formations (geological structure's delineation) beneath the surface. In the presence of a high-density distribution contour pattern coincides with a low susceptibility distribution contour pattern is suggested as the presence of relatively recent volcanic-rocks or younger rock-formations. Hence, magnetic methods proved its effectiveness in volcanic regions. In specific cases, the inclusion of paleomagnetic methods may be necessary for a comprehensive analysis.

The study area is located in the Majenang Regency, Central Java and is bounded within the coordinates 108.5º-109.0º E and 7.0º-7.5º S as shown by the red rectangle in Figure 1. In general, the study area is located in the middle part of Java Island. The study area is inferred to host promising geological resources, supported by the discovery of several oil and gas seepage site-locations [2], numerous hot-springs [3], and findings of mineral ore deposits, which proves the occurrences of mineralization in the area [4-6]. The situation leads the regional geology and subsurface structure in the study area becomes an intriguing subject for further investigation. Nevertheless, extensive volcanic-deposits covering the region pose challenges for exploration efforts. The utilization of magnetic and gravity methods in this study aims to delineate subsurface geological structures and identify the prospective area for geological resources modeling within the study area. A comprehensive understanding of the geological conditions in the study area will significantly enhance exploration efforts for geological resources within the region.

GEOLOGICAL SETTINGS

In the late Mesozoic to Cenozoic period, Java Island was formed. The magmatic arc on the island was shifted due to changes in the subduction zone. During the Cretaceous to Paleogene period (early Eocene), the magmatic arcs were situated in the northern part of West Java. Consequently, the Bogor depression zone evolved into a fore-arc basin [7-8], as shown in Figure 1. However, during the late Eocene to early Miocene, the magmatic arc was located in the southern part of Java Island, and was followed by a northward shift of the magmatic arc during the late Miocene to the Pliocene [9]. A significant change in structural pattern occurred in Java Island, transitioning from the Paleogene-Structure pattern, which is characterized by the northeast-southwest direction of the Meratus-Range to the Neogene-Structure pattern with a west-east orientation [10]. The most probable reasons for these major structural changes are the welding result of the Southwest-Borneo (SWB) and East-Java-West-Sulawesi (EJWS) blocks into the southeastern part of Sundaland as the detachment continental fragments of Gondwanaland [11-16]. Another result explained that the EJWS is divided into East-Java-Block (EJB) and Greater-Paternoster [17]. The extensional tectonics also occurred in the Makassar-Strait during Jurassic-Cretaceous period, which sequentially turned into Cretaceous-Subduction [18]. An oceanic crust (Paleo-Tethys) is suggested as a prior subduction beneath the Borneo before the Greater-Paternoster, which melted and raised the Schwaner-Range such that the extensional tectonics is triggered at that time. In general, Java exhibits four tectonic lineament patterns: the northeast-southwest orientation, known as the Meratus lineament; the north-south orientation, referred to as the Sunda lineament; the west-east orientation, known as the Java lineament; and the northwest-southeast orientation, commonly referred to as the Sumatran lineament [10].

Java Island is formed from several components, including the southeastern tip of the Eurasian-Continental-Plate, terrain accretions, and micro-continents derived from the Australian-Continental-Plate (Gondwanaland). In essence, Java Island is an extension of the southeastern tip of the Eurasian-Continent, formed through the amalgamation of several micro-continental landmasses (terranes). The collisions between the Sundaland margin and the micro-continents of Gondwanaland are believed to have occurred during the middle Cretaceous, with the suture boundary located at the Meratus-Range [19-20]. Several micro-continents (terranes) coalesced into a single landmass, giving rise to Java Island as an extension of the southeastern most of the Eurasian-Continent.

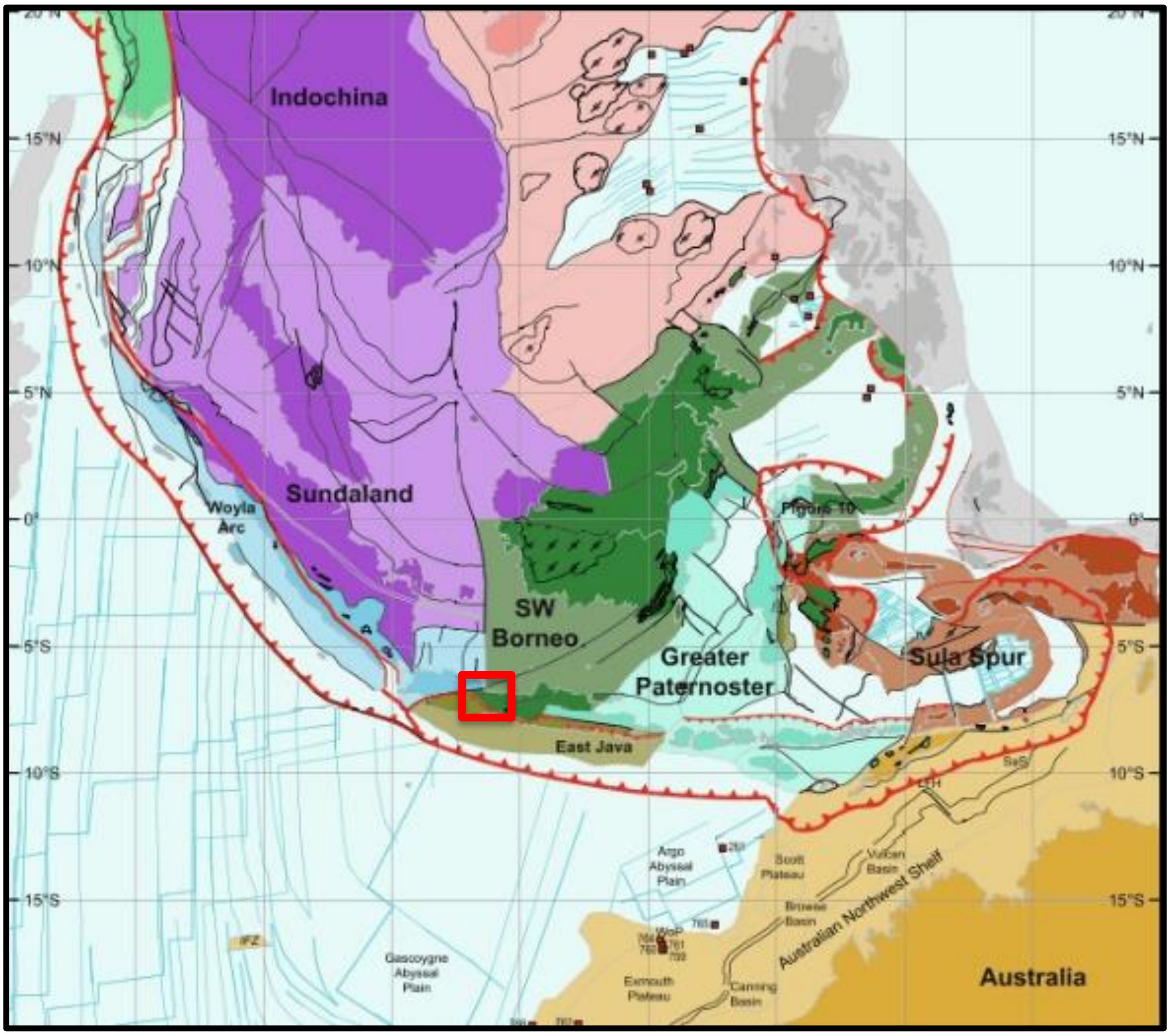

Figure 1. Tectonic settings of Indonesia from lithotectonic blocks and mega units [11-17] as the evidence of terrane accretions and terrane dispersions [21]. A red rectangle represents the study area presented in this work.

Other research related to volcanism suggests that the distribution of volcanoes on Java Island is not strictly from south to north but rather tends to be random, following the pattern of fault structures. These fault structures represent as the weak zones, which is penetrated by intrusive rocks and give rise to volcanoes in the area [22]. The fault structures and the adjacent volcanic lineament raise a hypothesis of the volcano-tectonic setting due to a transform or strike-slip fault in the study area. The Old Slamet-Volcano has been discovered in the vicinity of the study area, situated southwest of the current Slamet-Volcano [23]. Java Island is a volcanic island which is dominated by volcanic deposits across almost in all its areas. It is estimated that superimposed volcanism has occurred in Java Island, as evidenced by the discovery of Paleogene-aged volcanic-rocks adjacent to Neogene-aged volcanic-rocks [22]. The volcanic activity of Java Island commenced approximately 60 million years ago, aligning with the Paleogene-period, and has since increased in frequency, persisting until the present day [24]. This makes the Majenang area in Central Java is challenging for further study.

METHODS

The study used both magnetic and gravity methods to reduce the ambiguity factors during the data interpretation. Forward-modeling of synthetic data is carried-out in polar regions and equatorial-magnetic regions for comparison. Forward-modeling is conducted to determine the signatures or characteristics of both magnetic and gravity model responses due to horizontal faults (strike-slip fault). Forward modeling of TMI anomalies was performed with inclination angle parameters of 90º and -31.5967º to sequentially simulate TMI anomaly contour patterns in the polar regions and equatorial-magnetic regions of the Earth. The results of TMI data synthesis at the Earth's magnetic-equator are then transformed into RTP and RTE data anomalies as is generally done during magnetic data processing. The obtained results were compared with anomaly contour patterns of synthetic TMI in Earth's magnetic-polar regions. Such processing flow is conducted to recognize the characteristics of the filtering or transformation based on RTP or RTE.

The direct use of the field TMI dataset for the inversion process is carried-out under the assumption that the direction of the magnetization vector (remnant-magnetic) of the source-rock has the same direction with the regional magnetic-field-force-lines. The direct use of TMI data aims to reduce the appearance of any artifacts in RTP and RTE processing data due to incorrect parameters. The results of susceptibility modeling from field TMI data are then compared with the density modeling results based on field gravity data in the same area. Analysis and interpretation of the field data is carried-out using the model-solutions obtained from both magnetic and gravity data inversion modeling. In addition, the analysis and interpretation of field data also considers the geomorphological patterns of the study area and the distribution of geological formations dominated by the volcanic deposits.

Field Data Processing

The magnetic method essentially takes measurements of variations in Total Magnetic Intensity (TMI) on the Earth's surface. These variations are caused by distortions in the regional Earth's magnetic field as a result of differences in the magnetization of rocks below the Earth's surface. In other words, the magnetic properties of rocks below the Earth's surface are not homogeneous and will cause a TMI anomaly contour pattern. Variations in magnetized rocks can be caused by geological structures and lithological differences in subsurface rocks.

Equation 1 shows that a magnetic anomaly (ΔF) is the difference between the results of processing data from magnetic-field measurements (F^*) in Equation 2 with a reference magnetic field based on a mathematical model of the Earth's main magnetic field or commonly referred to as the International-Geomagnetic-Reference-Field (F_{IGRF}). There are several corrections in magnetic data processing, such as correction due to the read-difference (BB) between Base and Field, correction due to diurnal-variation (VH), correction due to the equipment-drift, and correction of IGRF. Here is the formulation of such magnetic anomaly data reduction.

$$\Delta F = F^* - F_{IGRF} \ , \qquad (1)$$

$$F^{*} = Field \pm VH \pm drift \pm BB \ , \tag{2}$$

$$BB = Base_{start} - Field_{start} \ , \tag{3}$$

$$VH = Base_{n} - Base_{start} \ , \tag{4}$$

$$drift = \frac{t_{f(n)} - t_{f\_start}}{t_{f\_end} - t_{f\_start}} \left[(Field_{end} - VH_{end}) - (Field_{start} - VH_{start}) \right] . \tag{5}$$

Magnetic surveys always require at least two magnetometers that function as Base and Field. Each measuring instrument has its own characteristics, so the readings between Base and Field are often different even though they are carried-out at the same location and time. This difference in readings should be considered in the magnetic data processing as a correction of the read-difference (BB) as shown in Equation 3. Diurnal-variation correction (VH) is required to determine the value of magnetic-field variation at the measurement site and to ensure no magnetic-storms occurs during measurement. The diurnal-variation (VH) is calculated on a synchronized time basis since the measurement began as shown in Equation 4. Where $Base_n$ is the result of a reading in *Base* that has the same time as a reading in $Field$. In most situation, the $Base_n$ value is obtained based on interpolation. The phenomenon of hysteresis in the sensor-coil will cause a shifting in readings. Therefore, it is necessary to correct the drift on the measuring instrument used as formulated in Equation 5. This kind of calculation will increase the accuracy of the measurement data of geomagnetic survey.

Reduction to Pole (RTP)

Earth can be described as a giant-magnet, where magnetic-field-force-lines of came-out in the Earth's magnetic north-pole and came-in or enter in the Earth's magnetic south-pole. This would cause each location on Earth's surface to have a magnetic-vector as shown in Figure 2a. Magnetic declination (D) is the angle in the flat plane between Earth's magnetic north-pole and the true-north. While magnetic inclination (I) is an angle formed by a magnetic field (magnetic-field-force-lines) against the horizontal plane of the Earth's surface.

The center of mass of the anomaly source in the gravity method will be correspond to the peak of the anomaly, but it is different anomaly behaviour in the magnetic method. The measurable pattern of Earth magnetic anomalies will be influenced by the magnetization vector of rocks and the regional magnetic field vector (IGRF) of the Earth at the measurement site. In case of the magnetization vector of rocks and the regional Earth's magnetic field are not vertically directional, a lateral shifts of the magnetic anomalies, or distortions, or even high-low polarity reversals may occurs as shown in Figure 2b.

The process of calculating RTP on the Fourier domain is expressed as follows [25]

$$F[\Delta T_r] = F[\psi_r] F[\Delta T] \ , \tag{6}$$

where:

$$F[\psi_r] = \frac{1}{\Theta_m \Theta_f} = \frac{|k|^2}{a_1 {k_x}^2 + a_2 {k_y}^2 + a_3 k_x k_y + i|k|(b_1 k_x + b_2 k_y)}, |k| \neq 0, \tag{7}$$

$$a_1 = \hat{m}_z \hat{f}_z - \hat{m}_x \hat{f}_x,$$

$$a_2 = \hat{m}_z \hat{f}_z - \hat{m}_y \hat{f}_y,$$

$$a_3 = -\hat{m}_y \hat{f}_x - \hat{m}_x \hat{f}_y,$$

$$b_1 = \hat{m}_x \hat{f}_z + \hat{m}_z \hat{f}_x,$$

$$b_2 = \hat{m}_y \hat{f}_z + \hat{m}_z \hat{f}_y.$$

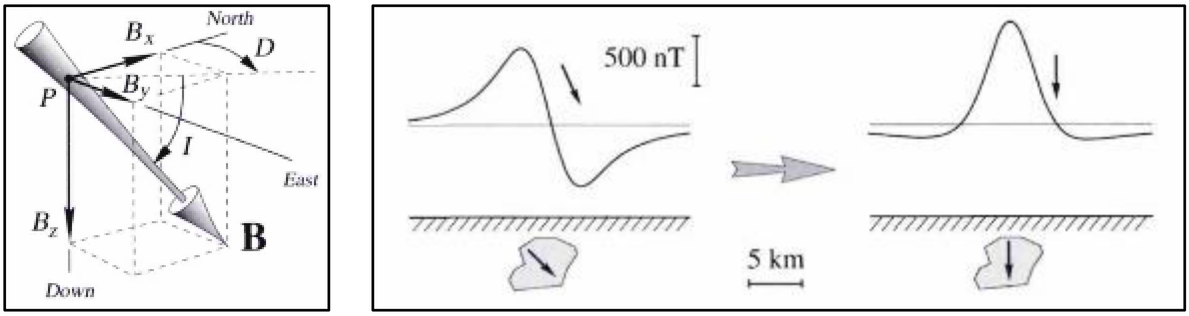

(a) (b)

Figure 2. a. Inclination (I) is the angle from F below the horizontal plane XY, positive value downward. Declination (D) is the azimuth value of the horizontal projection F, positive to the east [25].
b. Magnetic anomalies before (left) and after (right) Reduction to Pole (RTP).

Table 1. Parameters of inclination and declination angle values of the research area in Majenang, Central Java (https://www.ngdc.noaa.gov/)

Magnetic Field							
Model Used	: IGRF2020						
Latitude	: 7.24956275776° S						
Longitude	: 108.749961705° E						
Elevation	: 0.0 km Mean Sea Level						
Date	Declination (+E | -W)	Inclination (+D | -U)	Horizontal Intensity	North Comp (+N | -S)	East Comp (+E | -W)	Vertical Comp (+D | -U)	Total Field
2018-03-16	0.7950°	-31.5967°	38.209,6 nT	38.205,9 nT	530,2 nT	-23.503,7 nT	44.859,7 nT
Change/yr	-0.0281°/yr	0.1222°/yr	42.0 nT/yr	42.3 nT/yr	-18.2 nT/yr	86.5 nT/yr	-9.5 nT/yr

The ΔT notation in Equation 6 is the TMI anomaly of the magnetic method measurement as shown in Figure 2b (left), while the ΔT_r notation is a magnetic anomaly resulting from RTP operations where the direction of the source rock magnetization vector is in the same direction as the regional magnetic vector, which is vertical downward as shown in Figure 2b (right). The RTP filter parameters in Equation 6 and Equation 7 are denoted as $F(\psi_r)$. The RTP process will shift the magnetic anomaly laterally to the center of its anomaly source and make the anomaly pattern symmetrical according to the location and geometry of the source [25]. The RTP operation requires information related to the values of the inclination angle (I) and declination angle (D), which can be obtained based on the coordinates of the measurement location through the https://www.ngdc.noaa.gov/ site as shown in Table 1.

One procedure to overcome the problem of RTP stability in the equatorial-magnetic region is performing RTE. This technique will make the centre of the anomaly correspond to the source below the surface, but the anomaly contour pattern will be inverted to the RTP result and attracted in a west-east direction [25]. Alternative solutions compare to RTP or RTE can be done with an equivalent-source scheme, where TMI data can be used directly. The anomaly contour pattern of TMI is converted into a magnetic-band which is a subsurface discretization of one layer. Although equivalent-source is not the same as magnetic anomaly source rock, it can provide measurable magnetic anomaly model response. Inversion modeling is then performed on an equivalent distribution layer assuming that the magnetization vector is vertically directed.

Inverse Modeling

Modeling is done by discretizing the subsurface with amount number of rectangular-prisms. The magnetic field model-response from a rectangular-prism in the Cartesian coordinate system has been formulated [25]. The modeling result in magnetic method is influenced by two main factors: the magnetization of the rock (M) and the regional magnetic field of the Earth at the measurement site (F) as shown in Equation 8 and Equation 9. The equation gives the anomaly response of a total magnetic due to a rectangular-prism with an upper bound of z_1 and an infinite lower bound. By applying double calculations of Equation 8 and Equation 9, namely with the upper bound z_1 and the upper bound z_2, the difference between the two will give a pattern of total magnetic anomalies due to a rectangular-prism with the upper bound z_1 and lower bound z_2. Where C_m is the constant ratio between the magnetic permeability of free-air (μ_0) and 4π which in Systeme Internationale (SI) is $10^{-7}\ \frac{henry}{meter}$. While M is the magnetization parameter of rocks, $M = M\left(iM_x + jM_y + kM_z\right)$ and F are regional magnetic fields with components F_x , F_y , and F_z in the Cartesian Coordinate system. The equations are written as follows [25]

$$\Delta T = C_m M \Bigg[\frac{\alpha_{23}}{2}\, log\left(\frac{r-x'}{r+x'}\right) + \frac{\alpha_{13}}{2}\, log\left(\frac{r-y'}{r+y'}\right) - \alpha_{12}\, log(r+z_1) - \widehat{M}_x \widehat{F}_x\, arctan\left(\frac{x'y'}{x'^2+rz_1+z_1^2}\right) - \widehat{M}_y \widehat{F}_y\, arctan\left(\frac{x'y'}{r^2+rz_1+x'^2}\right) + \widehat{M}_z \widehat{F}_z\, arctan\left(\frac{x'y'}{rz_1}\right) \Bigg] \Bigg|_{x'=x_1}^{x'=x_2} \Bigg|_{y'=y_1}^{y'=y_2} ,, \tag{8}$$

where:

$$\alpha_{12} = \widehat{M}_x\widehat{F}_y + \widehat{M}_y\widehat{F}_x ,$$

$$\alpha_{13} = \widehat{M}_x\widehat{F}_z + \widehat{M}_z\widehat{F}_x ,$$

$$\alpha_{23} = \widehat{M}_y\widehat{F}_z + \widehat{M}_z\widehat{F}_y ,$$

$$r^2 = x'^2 + y'^2 + z_1^2 . \tag{9}$$

The solution of the inverse calculation utilizes the Tikhonov Regularization scheme, where the objective function [$\Phi(m)$] will minimize the misfit data [$\phi_d(m)$] and the model structure or norm-model [$\phi_m(m)$] simultaneously with the controlled equality or trade-off through the regularization parameter (β) as shown in Equation 10, Equation 11, and Equation 12. Determination of regularization parameters can be done using the L-Curve method [26]. The objective function equation of inversion modeling can be written as follows

$$\Phi(m) = \phi_d + \beta\phi_m , \tag{10}$$

$$\phi_d(m) = \frac{1}{2}\|W_d(F[m] - d_{obs})\|_2^2 , \tag{11}$$

$$\phi_m(m) = \frac{1}{2}\|W_m\left(m - m_{ref}\right)\|_2^2 . \tag{12}$$

Where $F[m]$ in Equation 11 is a forward modeling of the model parameter m which produces calculated data (d_{calc}). The d_{obs} parameter is the measurement data, while W_d is the weight matrix to accommodate the uncertainty or erroneous in the data acquisition or measurement (standard-deviation or noise). The m_{ref} parameter represents the reference model within the calculation process, but it can also be zero [27]. Reference models play a role when involving geological concepts in the calculation process.

RESULT AND ANALYSIS

Synthetical Data Modeling

Forward modeling of magnetic methods is needed to understand the implementation characteristics of applying RTP and RTE filters to TMI datasets. The subsurface model consists of two identical prism models with the difference just in its lateral position, in such a way to represent the presence of strike-slip faults. The numerical parameters and geometry of the model are shown in Table 2. In general, the two prism models are the same and identical, differing only laterally as shown in Figure 3a. Figure 3b is a synthetic model response using 90º inclination angle, which simulates the results of TMI measurements in the north-polar region (TMI-pole) where the direction of the vertical magnetic field is entering the Earth. The next modeling is also carried-out on the Earth's magnetic-equatorial region (TMI-eq) with an inclination angle of -31.5967º and its model response is shown in Figure 3c. The value of the inclination angle was chosen to simulate the anomaly contour pattern of TMI in the study area. The RTP calculation results from TMI anomaly data on the Earth's magnetic equator (TMI-eq) or previous result in Figure 3c are shown in Figure 3d. Forward modelling of gravity method is adapted from our previous work, which yield comparable results [28].

Tabel 2. Parameters of synthetic models

	Prism #1 (m)		Prism #2 (m)	
X	241572.08	254679.20	250646.24	263753.36
Y	9179240.5	9197381.4	9197381.4	9215522.4
Z	-2519.565	-4535.217	-2519.565	-4535.217
Sc.	5.000000 e-3		5.000000 e-3	

Forward modeling demonstrates that the TMI anomalies does not reflect the geometric shape of the anomaly source at all (Figure 3c) compare to the RTP results (Figure 3d). The utilization of RTP filter in certain situation provides artificial artifacts in the processed data, especially when the parameters used are incorrect. As the result, the filtered data will be stretched in the north-south direction. The anomaly contour pattern of magnetic RTP calculation results that are stretched in the north-south direction can be corrected by applying Amplitude Correction Inclination (ACI) using Oasis Montaj software. However, the determination of such parameters is still subjective. The same thing is found in the application of RTE computing, where the processed data will be stretched in the west-east direction [25]. Noteworthy, defining the parameters during applying RTP and RTE should be done carefully, except it will provides a result with artificial artifacts to the data. If this so, such artifact contour patterns appear in the processing must be observed and not to be interpreted geologically.

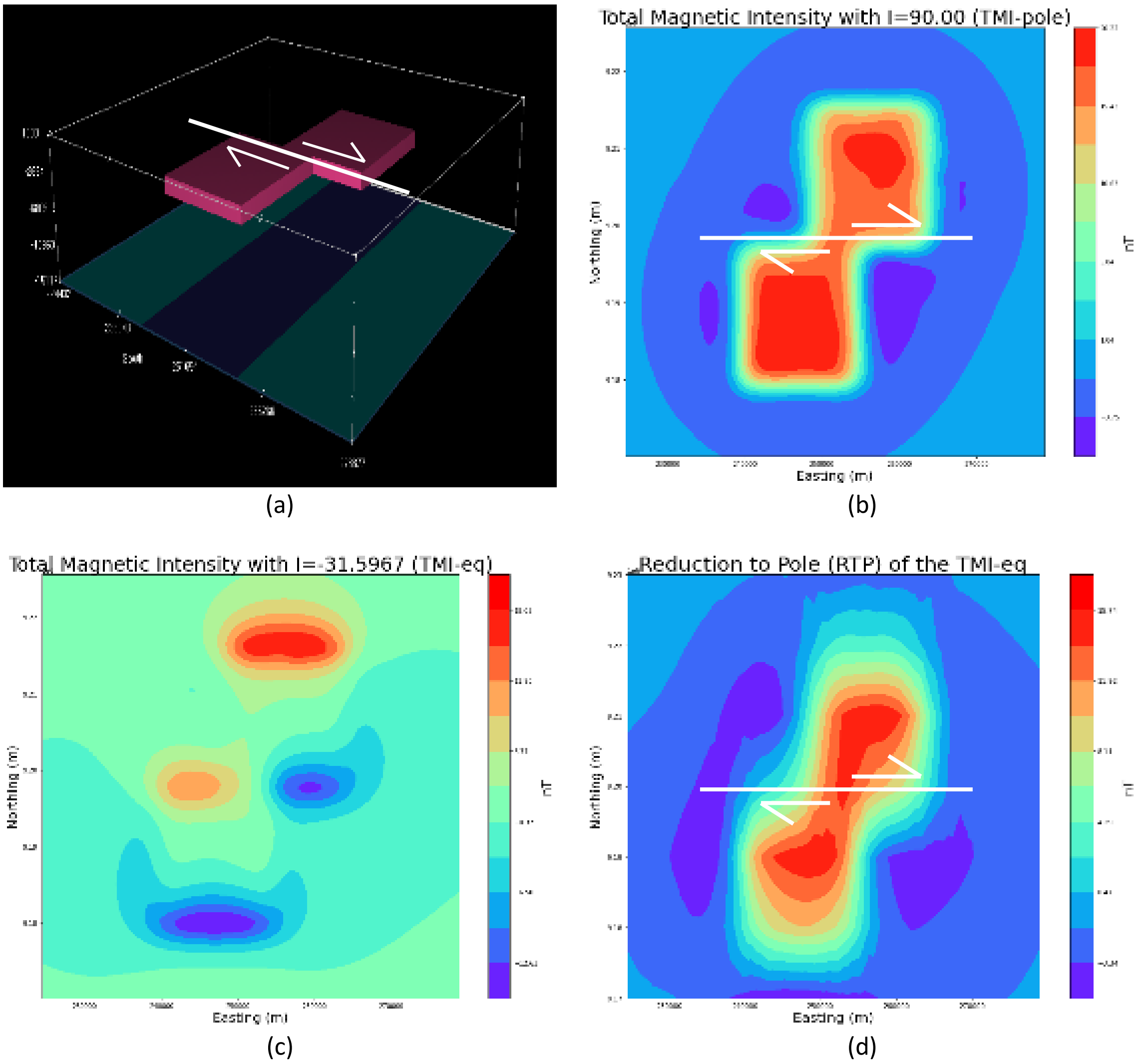

Figure 3. Forward modelling of Total Magnetic Intensity (TMI) response based on two identical prisms with uniform susceptibility values such as to simulate strike-slip faults (a). Model response is calculated at the polar regions (TMI-pole) with an inclination angle of 90° (b), and at the Earth's magnetic-equator region (TMI-eq) with an inclination angle of -31.5967° (c). The Reduction to Pole (RTP) is applied to Total Magnetic Intensity (TMI-eq) data in the Earth's magnetic-equator region (c) and yield RTP anomaly contour patterns (d). The strike-slip fault is marked using white line on the figures.

Direct use of the TMI anomaly for data processing becomes an alternative solution to avoid any artificial artifacts on the data after applying of the RTP and RTE filters due to incorrect parameters. Inversion modeling was performed using synthetic magnetic anomaly dataset in the Earth's magnetic-equator (TMI-eq) with an inclination angle of -31.5967°. The results of the synthetic data inversion are shown in Figure 4, which consists of smoothness regularization (Figure 4a) and compactness regularization (Figure 4b) implementations. It is demonstrated that the inversion method yields susceptibility model that is close to a given synthetic model (Figure 3a). Compactness regularization provides more focused result at the center of the anomaly source compare to the smoothness regularization. Inverse modeling on the synthetic data using a direct use of TMI anomaly yields model-solutions that resolved the given synthetic model. Hence, the inversion scheme based on the direct use of TMI data can be applied to field data. A complete synthetic inverse modeling work consisting both magnetic and gravity results can be referred to another previous published work [29].

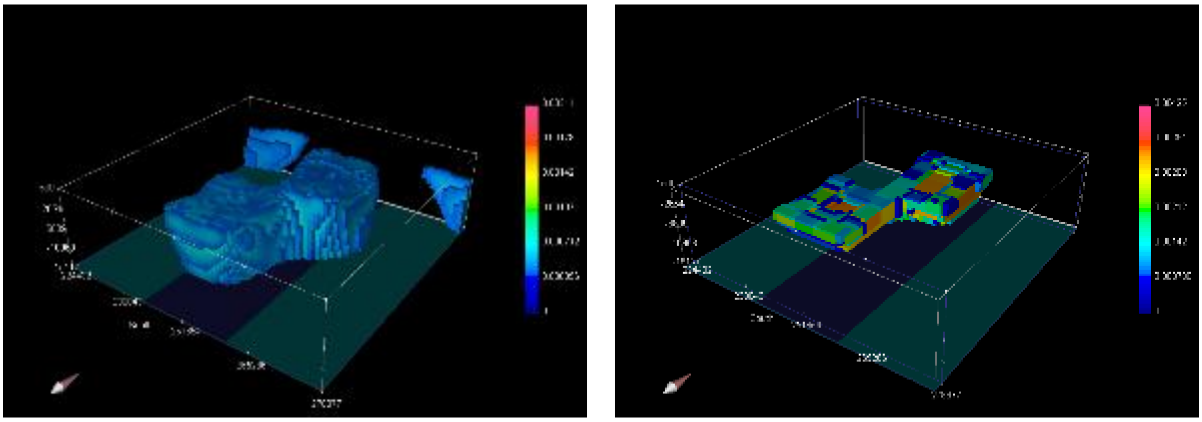

(a) (b)

Figure 4. Inversion results of the synthetic Total Magnetic Intensity (TMI-eq) data anomaly with an inclination angle of -31.5967° using smoothness regularization (a) and compactness regularization (b), which is adapted from our previous work [29].

Field Dataset Implementation

TMI data inversion results from the field measurements of the TMI dataset in the Majenang area are shown in Figure 5, Figure 6, and Figure 7. The distribution of near-surface susceptibility distribution along with the measurement points of both the magnetic and gravity methods are superimposed with the geological maps in the study area [29] as shown in Figure 5. The red dot indicates the gravity measurement point locations, while the black dot indicates the magnetic measurement point locations. A lateral comparison between the susceptibility model-solution and the density model-solution in the study area is shown in Figure 6. Figure 7 shows a visualization of geometric comparisons between solutions of the susceptibility model and the density model.

According to the subsurface model-solution obtained from the two methods, the offset or net-slip is clearly identified in the northwest–southeast alignment direction as shown in Figure 6 and Figure 7. The susceptibility model-solution is shown in Figure 6a and Figure 7a, while the density model-solution is depicted in Figure 6b and Figure 7b [28-29]. The shifting pattern is interpreted as the Pamanukan-Cilacap Dextral Strike-Slip Fault, which becomes the part of the Pamanukan-Cilacap Fault Zone (PCFZ) [31]. The Pamanukan-Cilacap Dextral Strike-Slip Fault is estimated to be a deep-seated fault with the inferred depths of about 3000 up to 5000 m below the surface and aligned with a Sumatran lineament or northwest-southeast orientation (Figure 7). The PCFZ is thought to be relatively perpendicular to the folding structures with the northeast-southwest alignment (Meratus lineament patterns) which is formed earlier during the docking-period at the time of the formation of Java Island. These folding structures inferred to be existed but it is covered by the volcanic sedimentation sequences. Hence, the situation leads as a challenge in subvolcanic explorations. The circular-pattern anomaly found as the high-susceptibility model and high-density model are interpreted as the part of ring-faults or caldera-rims of the Majenang Ancient-Volcanic-Caldera (Figure 6 and Figure 7).

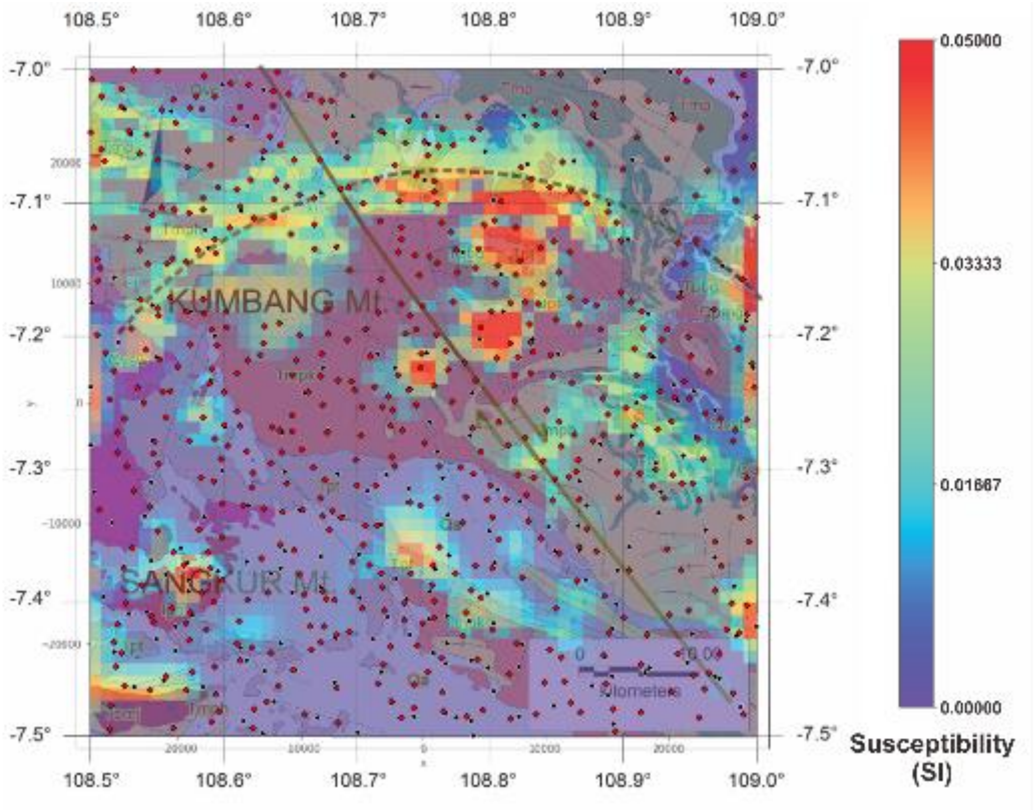

Figure 5. Distribution of the near-surface susceptibility model in Majenang and its surrounding areas superimposed with the Geological Map of Majenang Sheet scale 1:100.000 [30]. The red dot indicates the location of the gravity measurement points, while the black dot indicates the location of the magnetic method measurement points.

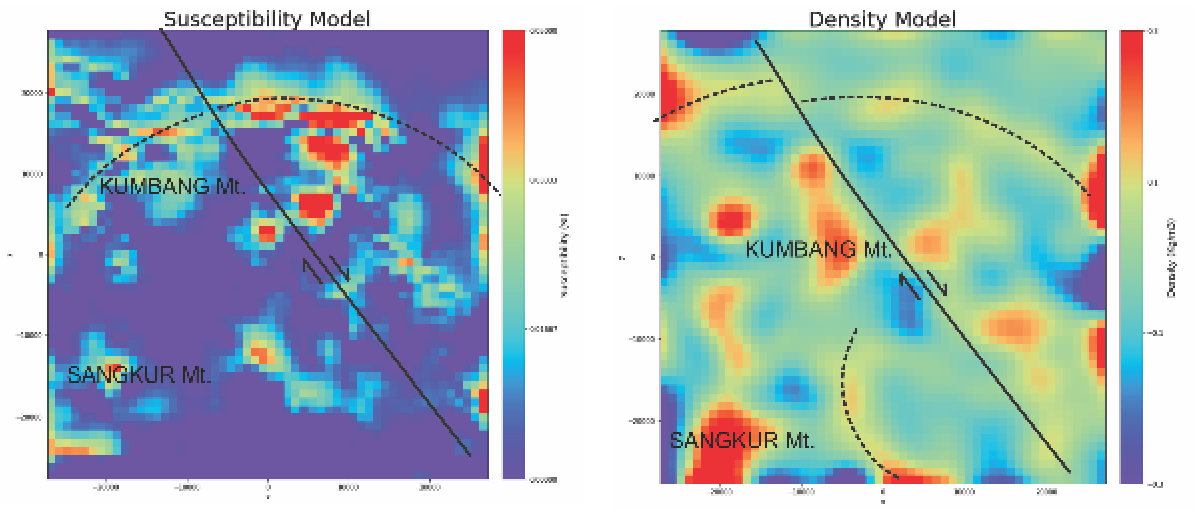

(a) (b)

Figure 6. Comparison of the results obtained from the TMI data inversion in the form of subsurface susceptibility distribution (a) and gravity data inversion results [28] in the form of subsurface density distribution (b) at the same research location in Majenang, Central Java.

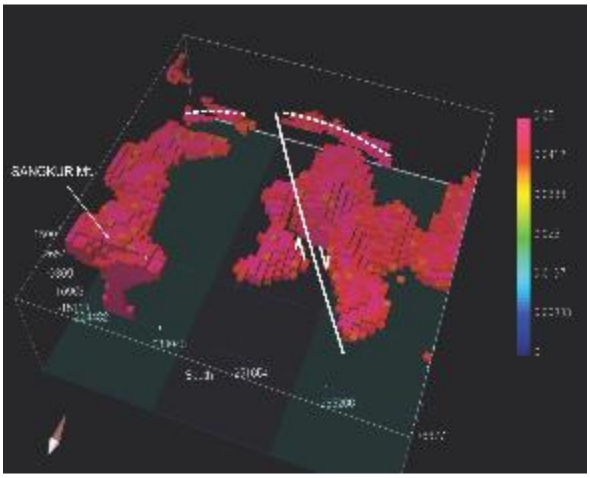

(a)

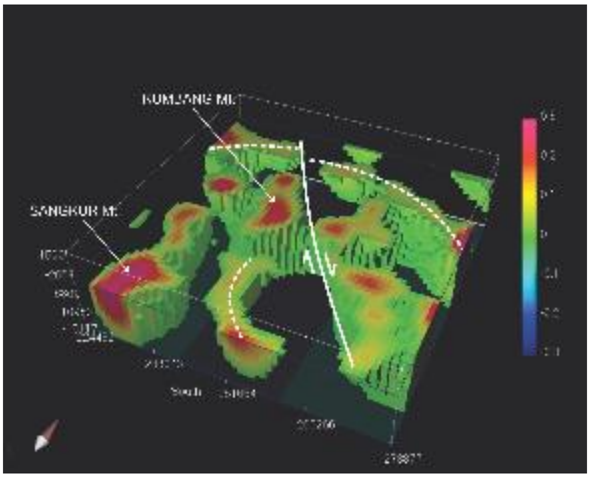

(b)

Figure 7. Visualization of anomaly source geometry beneath the surface in the form of susceptibility model (a) and density model (b) in the Majenang area, which shows the compatibility results between magnetic and gravity methods. These results are adapted from our previous work [29].

In addition to these anomaly patterns, there are also high-susceptibility anomalies and high-density anomalies in the form of separate spots (Figure 6). These anomaly patterns were interpreted as intrusive rock bodies in the study area. One of the intrusive rock bodies is located around Mount-Sangkur. This location corresponds to the high-susceptibility and high-density. However, the intrusive rocks located on Mount-Kumbang exposes different manner, this location has a high-density anomaly pattern coincides with a low-susceptibility anomaly distribution. The difference that arises is thought to be related to the process of magma cooling, where the intrusion rocks of Mount-Sangkur are thought to have cooled first (older) compared to the intrusive rocks of Mount-Kumbang.

The existence of intrusive rocks around the Pamanukan-Cilacap Fault Zone (PCFZ) location becomes the evidence of magmatism activity in the study area. This phenomenon shows that the emergence of volcanoes in the study area is related to the PCFZ, which becomes the weak zone such that it is easily penetrated by intrusive rocks and raised volcanoes around it. The phenomenon is inferred as a volcano-tectonic system in the study area as the transform boundaries that involves shifting past tectonic plates. Volcanic activity may develop along these boundaries, in addition to as is common in subduction zones. The volcano-tectonic order can be recognized by the straightness of several volcanic eruption points called volcanic-lineament. This study inferred the Cipari anticline as the eruption point, which is shifted by the fault within the fault zone (PCFZ) instead of a folding structure as defined in the previous result [32]. Thus, the solution of the subsurface susceptibility model based on geomagnetic data (Figure 6a and Figure 7a) corresponds to the density model from the gravity data (Figure 6b and Figure 7b) and interpreted as an ancient volcanic caldera in the study area.

The next process is to validate the susceptibility model solution obtained based on the inversion modeling scheme. The calculation input data is in the form of TMI, so a comparison is needed between TMI data from field work measurements (TMIobs) and TMI calculations from the inversion process (TMIcalc) as a benchmark for success in the inversion modeling. In general, the TMIcalc contour pattern is close to the TMIobs contour pattern as shown in Figure 8. The difference is due to uncertainty during measurements (standard-deviation or noise) and due to the assumption that the direction of the rock's magnetization (remnant-magnetic) has the same with the direction of regional magnetic-field-force-lines in the study area. Finally, the inversion modeling based on TMI data from the field measurements (TMIobs) is sufficient to be used in the process of interpreting subsurface conditions in the research area. The same comparison procedure has been conducted in the gravity datasets from the previous work [28].

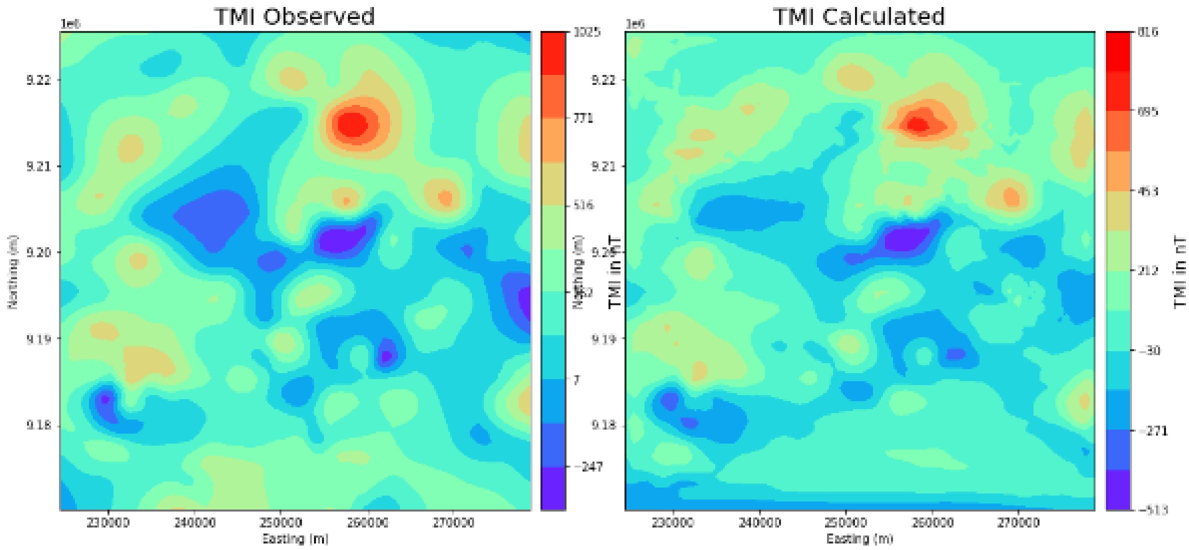

Figure 8. Comparison of magnetic data in the form of Total Magnetic Intensity measurement results (TMIObs) and Total Magnetic Intensity data of the modeling results from the susceptibility model solution obtained (TMICalc).

DISCUSSION

Nowadays, proving the existence of an ancient volcanic environment poses a challenge for geoscientists, which raise debates. However, the presence of geological manifestations discovered in the study area guides a possibility regarding to the existence of this geological feature becomes plausible and logical. Here are some approaches that can serve as indicators of the volcanic environment in the study area: [1] An adjacent finding both mineralization zones in Cihonje, which has been transform into a People-Gold-Mine; [2] and the existence of the hot-spring in Cipari anticline, which has turned into a hot-water swimming pool in the area. This hot-water has been analyzed and identified derived from the meteorite-water and implies the existence of a heat-source around the study area; [3] Findings of the Old Slamet-Volcano which is located at the southwestern part of the recent Slamet-Volcano. Further, it is proved the theory of superimposed volcanism in Java Island; [4] and the last is from geophysical point of view, which discovers a circular anomalies pattern based on gravity residual and magnetic RTP datasets. Manifestation of the mineralization zones and the hot-springs of Cipari proved that the study area is highly correlated with the volcanic environment. According to the Digital Earth Model (DEM) analysis, it is proposed that the Cipari Ridge is defined as the eruption center, which has been shifted due to the Pamanukan-Cilacap Fault Zone (PCFZ) activities. Cipari anticline is rising due to volcanism activity and is shifting due to the tectonic activity in the area controlled by the PCFZ. Such phenomenon is known as the volcano-tectonic setting in the study area.

CONCLUSION

The Equivalent Source of 3-D magnetic inversion modeling scheme using Total Magnetic Intensity (TMI) data offers an alternative solution regarding the stability issue in RTP calculations. The method able in overcoming the appearance of intermittent artificial artifacts which might raise due to the incorrect implementation of the Reduction to Pole (RTP) and Reduction to Equator (RTE) computations methods. Inversion processes significantly depend on the inclination and declination angle values determination within the data processing. The analysis of field dataset reveals an offset or shifting, which is interpreted as the Pamanukan-Cilacap Dextral Strike-Slip Fault as the part of the Pamanukan-Cilacap Fault Zone (PCFZ). Additionally, a circular anomaly pattern identified in the study area is inferred as the perimeter of an ancient-volcanic-caldera, possibly comprising a ring-fault or caldera-rims. Thus, the research area was proposed as an ancient-volcanic-caldera of Majenang. The high-susceptibility zone corresponds to the high-density zone and the outcrop of the intrusive rock of Mount-Sangkur, so that the intrusive rock is interpreted as the volcanic body of Mount-Sangkur. Meanwhile, there is a low-susceptibility zone that corresponds to the high-density zone around Mount-Kumbang, this shows that the intrusion body of Mount-Kumbang is relatively younger than the intrusion rocks in the Mount-Sangkur area. There are several other intrusive bodies identified around the Pamanukan-Cilacap Fault, which show that PCFZ becomes a weak zone that is penetrated by intrusive rocks and raises to another new volcanoes as a volcano-tectonic system in the Majenang area and its surroundings. One of the characteristics of the volcano-tectonic system is the straightness of several volcanic eruption points called volcanic-lineament.

ACKNOWLEDGMENTS

We extend our sincere gratitude to the Centre for Geological Survey, Geological Agency, Ministry of Energy and Mineral Resources (MEMR) and the Research Center for Geological Resources (RCGR), National Research and Innovation Agency (NRIA) of the republic of Indonesia for their support and contributions, which have provided valuable research opportunities. Additionally, we appreciate the reviewers for their invaluable suggestions that have significantly contributed to the improvement of this work.

REFERENCES

1 Hutubessy, S. 2008. Pola Cekungan Dan Struktur Bawah Permukaan Ditinjau Dari Hasil Analisis Gaya Berat Dan Magnet di Daerah Banjarnegara, Jawa Tengah Bagian Selatan, J. Geol. dan Sumberd. *Miner*, *18*(4), 265-278.

2 Armandita, C., Mukti, M. M., & Satyana, A. H. 2009. Intra-Arc Trans-Tension Duplex of Majalengka to Banyumas Area: Prolific Petroleum Seeps and Opportunities in West-Central Java Border, Indones. Pet. Assoc. Thirty-Third Annu. Conv. Exhib. May 2009.

3 Iswahyudi, S., Permanajati, I., Setijadi, R., Zaenurrohman, J. A., & Pamungkas, J. A. 2020. The Origin of Geothermal Water Around Slamet-Volcano - Paguyangan - Cipari, Central Java, Indonesia, J. Geosci. Eng. Environ. *Technol*, *5*(4), 206–210.

4 Indarto, S., Sudarsono, S., Setiawan, I., Permana, H., Al Kausar, A., Yuliyanti, A., & Yuniati, M. D. 2014. Batuan Pembawa Emas Pada Mineralisasi Sulfida Berdasarkan Data Petrografi Dan Kimia Daerah Cihonje, Gumelar, Banyumas, Jawa Tengah. *RISET Geologi dan Pertambangan*, *24*(2), 115-130.

5 Sudarsono, Indarto S., Setiawan I., Yuniati, M. D. & Yuliyanti A. 2010. Model Genesa Mineralisasi Hidrotermal Daerah Cihonje, Kabupaten Banyumas, Jawa Tengah. Prosiding Pemaparan Hasil Penelitian Puslit Geoteknologi-LIPI 2010. 33 – 42.
6 Chusni, A. & Puswanto, E. 2009. Alterasi dan Mineralisasi di Daerah Pertambangan Rakyat Cihonje, Kecamatan Gumelar, Kabupaten Banyumas Berdasarkan Analisis Kimia dan Mineralogi. Prosiding Pemaparan Hasil Penelitian Puslit Geoteknologi – LIPI 2009. 19-28.
7 Katili, J. A. 1973. GEOCHRONOLOGY OF West INDONESIA AND ITS IMPLICATION ON PLATE TECTONICS, Techtonophysics, 19, 195-212.
8 Katili, J. A. 1975. Volcanism and plate tectonics in the Indonesian island arcs, Tectonophysics, 26(3-4), 165-188.
9 Soeria-Atmadja, R., Maury, R. C., Bellon, H., Pringgoprawiro, H., Polve, M., & Priadi, B. 1994. Tertiary magmatic belts in Java. *Journal Southeast Asian Earth Science, 9*(1-2), 13-27.
10 Bachri, S. 2014. Pengaruh Tektonik Regional Terhadap Pola Struktur dan Tektonik Pulau Jawa, Geol. dan Sumberd. *Miner, 15*(4), 215-221.
11 Hall, R. 2012. Late Jurassic-Cenozoic reconstruction of the Indonesian region and the Indian Ocean. Tectonophysics 570-571(2012), 1-41.
12 Metcalfe, I. 1996. Pre-Cretaceous evolution of SE Asian terranes. Tectonic Evolution of Southeast Asia, Geological Society Special Publication, 106, 97-122.
13 Metcalfe, I. 2011. Tectonic framework and Phanerozoic evolution of Sundaland, Gondwana Research, 19(1), 3-21.
14 Metcalfe, I. 2013. Gondwana dispersion and Asian accretion: Tectonic and Palaeogeographic evolution of eastern Tethys, Journal of Asian Earth Sciences, 66(2013), 1-33.
15 Smyth, Helen R., Hall, Robert., Nichols & Gary, J. 2008. Cenozoic volcanic arc history of East Java, Indonesia: The stratigraphic record of eruptions on an active continental margin. *The Geological Society of America, Special Paper 436: Formation and Application of the Sedimentary Record in Arc Collision Zones, 243*6(10), 199-222.
16 Batara, B. & Xu, C. 2022. Evolved Magmatic Arcs of South Borneo: Insights into Cretaceous Slab Subduction. Gondwana Research, 111(2022), 142-164.
17 Advokaat, Eldert L., van Hinsbergen, Douwe J. J. 2024. Finding Argoland: Reconstructing a microcontinental archipelago from the SE Asian accretionary orogen. Gondwana Research 128, 161-263.
18 Monnier, C., Polve, M., Girardeau, J., Pubellier, M., Maury, R. C., Bellon, H., Permana, H., 1999. Extensional to Compressive Mesozoic Magmatism at the SE Eurasia Margin as Recorded from the Meratus Ophiolite (SE Borneo, Indonesia). Geodinamica Acta, 12(1), 43-55.
19 Wakita, K., Miyazaki, K., Zulkarnain, I., Sopaheluwakan, J., & Sanyoto, P. 1998. Tectonic implications of new age data for the Meratus Complex of south Kalimantan, Indonesia, Isl. Arc, 7(1-2), 202-222.
20 Hall, R., Clements, B., & Smyth, H. R. 2009. Sundaland: basement character, structure and plate tectonic development, Proc. Indones. Pet. Assoc. 33rd Annu. Conv., on July, 1-27.
21 Satyana & Awang, H. 2003. Accretion and dispersion of southeast sundaland: the growing and slivering of a continent. Proceedings of Joint Convention Jakarta, Indonesia, 2003
22 Bronto, S. 2006. Fasies gunung api dan aplikasinya, Indones. J. Geosci., 1(2), 59-71.
23 Sutawidjaja, I. S., & Sukhyar, R. 2009. Cinder cones of Mount Slamet, Central Java, Indonesia, Indones. J. Geosci., 4(1), 57-75.
24 Bachri, S. 2017. Pengaruh Kegiatan Tektonik & Vulkanisme Terhadap Sedimentasi Endapan Paleogen-Neogen di Cekungan Serayu, Jawa. LIPI Press.
25 Blakely, R. J. 1995. Potential Theory in Gravity and Magnetic Applications. Cambridge University Press.
26 Zhdanov, M. S. 2002. GEOPHYSICAL INVERSE THEORY AND REGULARIZATION PROBLEMS.
27 Menke, W. 1984. Geophysical Data Analysis: Discrete Inverse Theory.
28 Handyarso, A. 2022. Ring-fault delineation of an ancient volcanic caldera based on 3-D gravity inverse modeling in the Majenang region, Indonesia, Kurvatek, 7(2), 103-114.

29 Handyarso, A. 2022. Caldera-Like Delineation and Geological Resources Identification of Majenang Area, Indonesia by Gravity and Magnetic Data Inversions. IOP Conference Series: Earth and Environmental Science 1227 (012027).

30 Kastowo. 1975. Geologic Map of The Majenang Quadrangle, Java Scale: 1:100.000. Bandung: Pusat Penelitian dan Pengembangan Geologi.

31 Muchsin, N., Ryacudu, R., Kunto, T. W., Budiyani, S., Yulianto, B., Wiyanto, B., ... & Riandra, F. 2002. Miocene hydrocarbon system of the Southern Central Java region. In *Proceeding of 31st Annual Convention of Indonesian Association of Geologists*. 31st Annual Convention, 58-67.

32 Lunt, P., Burgon, G. & Baky, A. 2009. The Pemali Formation of Central Java and Equivalents: Indicators of Sedimentation on an Active Plate Margin. *Journal of Asian Earth Sciences, 34*, 100-113.